

## Flexible and Printed Electronics



### PAPER

# Glucose sensing and hybrid instrumentation based on printed organic electrochemical transistors

RECEIVED  
28 August 2019

REVISED  
6 November 2019

ACCEPTED FOR PUBLICATION  
18 December 2019

PUBLISHED  
16 January 2020

Rakesh Rajendran Nair 

Saralon GmbH, Chemnitz, Germany

E-mail: [rakesh.nair@saralon.com](mailto:rakesh.nair@saralon.com)

**Keywords:** printed transistor, screen printing, hybrid circuit, glucose, organic electrochemical transistor (OECT)

### Abstract

This report presents the design and fabrication of a fully open-air printed organic polymer biosensor for detecting hypo/hyperglycaemia among humans with a fully integrated inorganic measurement and notification circuitry fabricated on a single flexible plastic substrate. The sensor is based on the electrochemical doping and de-doping of the degenerately doped organic semiconductor Poly (3,4-ethylenedioxythiophene) poly(styrene sulphonate) (PEDOT:PSS). The printed sensor reported herein, demonstrated sensitivity between 0.001 and 10 mM glucose concentrations utilizing a PEDOT:PSS gate, hence allowing for saliva-based, non-invasive glucose measurements. Transimpedance amplification and data processing circuitry for a prototype measurement and notification system was developed using three inexpensive chips: On Semiconductor's CAT102 precision regulator, Texas Instruments' LM358DR op-amp and Microchip's-ATMEGA328PB-AUR, all integrated on the same polyethylene terephthalate substrate using screen-printed Ag interconnects and vertically conducting anisotropic glue to demonstrate the system's practicability as a cheap, self-reliant, battery powered bio-sensing module. To demonstrate the efficacy of the system 'as is', no redox mediators to amplify the biosensor response were employed.

## 1. Introduction

212.4 million people across the world (about half of all people afflicted with Diabetes) are unaware and undiagnosed of their condition, with 84.5% of all undiagnosed cases stemming from low- and middle-income countries [1]. A pressing need is felt for a cheap, use-and-throw sensor capable of simply alerting the user of high (or low) levels of glucose such that they may subsequently seek out professional health-care especially in countries with relatively exorbitant costs of commercial amperometric glucose monitors.

OTFTs can be divided primarily into organic field effect transistors and organic electrochemical transistors (OECTs) based on differences in device structure and operational principles. Much effort has been put into the development of OECTs for biosensing applications in the past few years primarily due to their low operational voltages which allow for the real time sensing of compounds in aqueous electrolytes and their sensitivity to both electrons and ions which are the primary charge carriers in biological functions.

OECTs have been implemented in several sensing applications, like glucose [2, 3], pH [4], bacteria [5], Lactate [2], DNA [6], Ascorbic Acid [7] among others [8, 9]. The existing literature makes it clear that the biocompatibility of PEDOT:PSS and the availability of cost-effective deposition methods such as screen printing have allowed for an impressive amount of flexibility in terms of OECT architecture, sensing techniques and targeted analytes [8, 9].

No doubt, over the years PEDOT:PSS has become a commercially available, air stable benchmark material for OECT fabrication. However, not a lot of work has gone into the potential commercialization of OECT sensors as cheap, disposable test strips capable of detecting and notifying analyte concentrations exceeding medically harmful thresholds to the user. In this study, focus has been on the development of a simple PEDOT:PSS source-drain OECT architecture for the in-vitro sensing of glucose in saliva such that cheap, easy to manufacture sensor strips can be fabricated in order to detect hypo/hyperglycaemia in humans.

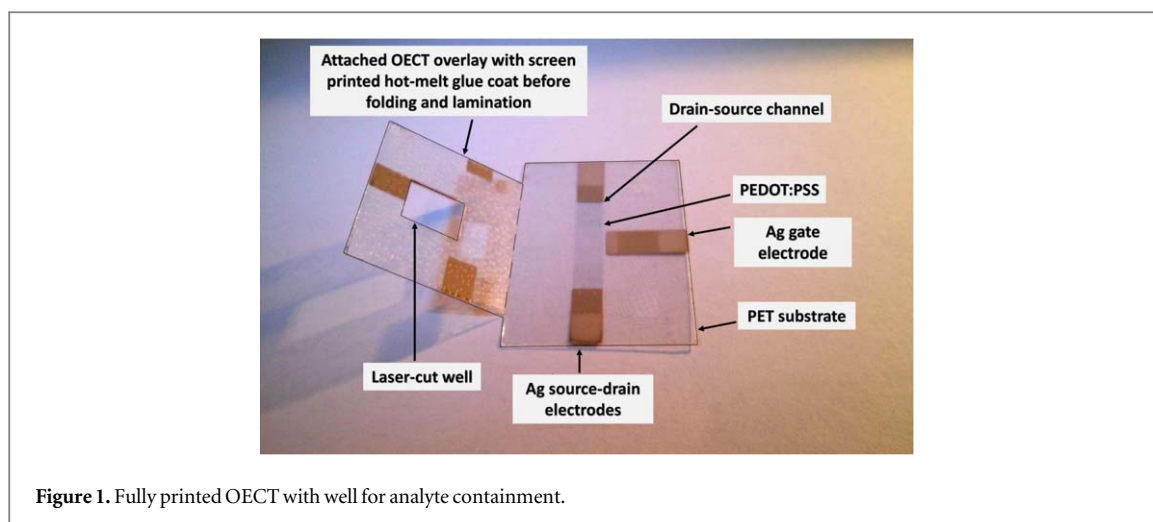
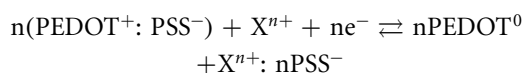


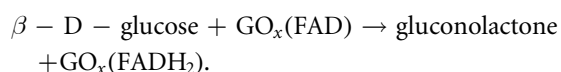
Figure 1. Fully printed OEET with well for analyte containment.

The sensor is based on the well-known enzymatic interaction between Glucose Oxidase ( $GO_x$ ) and  $\beta$ -D-glucose [10–13] within a phosphate buffer saline (PBS) generating hydrogen peroxide ( $H_2O_2$ ). The oxidation of  $H_2O_2$  creates electrons in direct proportion to the glucose concentration. This changes the potential-drop across the electrolyte and is accompanied by an ion influx into the semiconducting channel which manifests as an electronically measurable modulation of the drain current. Effectively, the application of a positive gate voltage ( $< 1$  V) in PEDOT:PSS based OEETs causes a concomitant drop in drain current from the cations in the electrolyte drifting into the PEDOT:PSS channel [14] and dedoping it as shown in the following reaction:

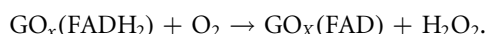


Additionally, the following reactions occur within the sensor for the measurement of glucose:

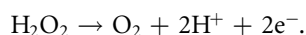
The  $\beta$ -D-glucose added in the electrolyte triggers the sensor by first reacting with oxidized glucose oxidase as in the following reaction to generate gluconolactone while glucose oxidase gets reduced:



This reduced glucose oxidase being an enzyme acts as a catalyst and cycles back to its oxidized form in the presence of oxygen to generate hydrogen peroxide:



The peroxide generated in the solution gets oxidized at the gate electrode to release water and two electrons that reduce the potential drop at the electrolyte-gate interface:

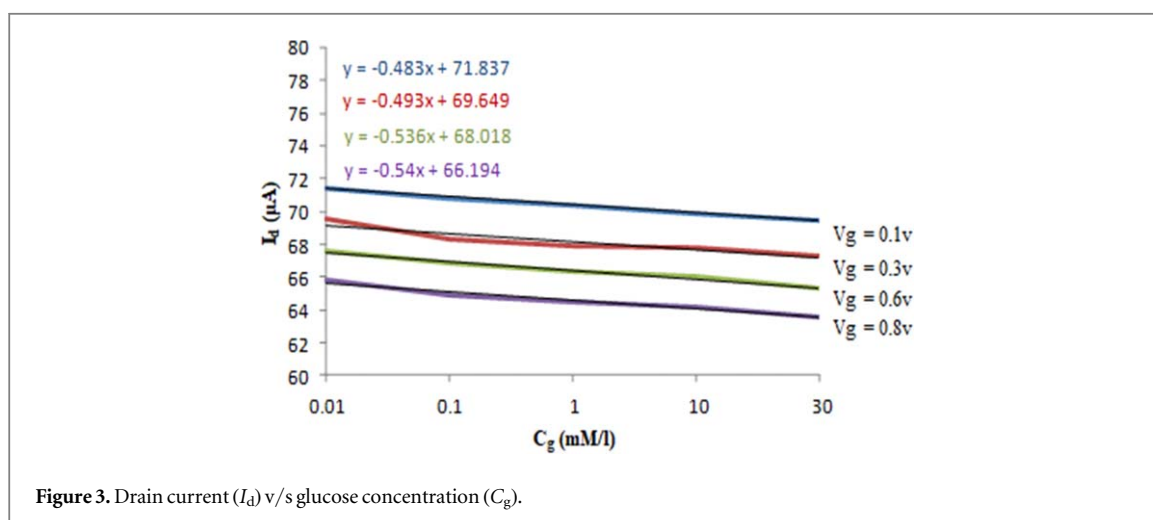
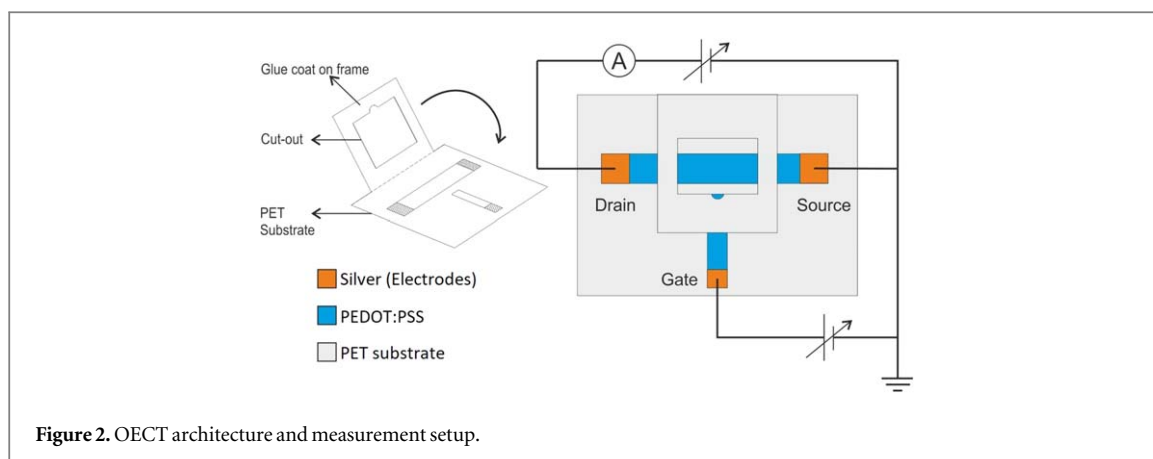


These charges enter the semiconductor at a quantity proportional to the amount of oxidation that occurs at the gate terminal, which, in-turn, depends

on the concentration of glucose present. Thus when the channel gets de-doped because of the cations in the electrolyte entering it and dropping its conductivity by way of the electrochemical mechanism and the ion-leveraged mechanism [14], the effective drop in current is directly proportional to the glucose concentration in the analyte of interest such as blood or saliva. It is to be noted that although the sensor was observed to be sensitive to previously reported blood glucose concentrations [15], focus was put exclusively on the measurement of glucose concentrations concurrent with human saliva.

## 2. Experimental procedure

Figure 1 demonstrates the elemental construction of the glucose sensor. The sensor was fabricated on a plasma treated 100  $\mu\text{m}$  thick Polyethylene terephthalate substrate via screen printing. A semi-automatic screen printer (Ekra X4) was used to deposit the electrodes and circuit interconnects along with an anisotropic, vertically conducting, glue for affixing the CMOS components. In order to avoid substrate deformation the polyethylene terephthalate (PET) sheets were preheated at 120  $^\circ\text{C}$  for 15 minutes. The PEDOT:PSS source-drain channel was deposited with an effective area of 10 mm  $\times$  5 mm. A mesh size of 90–40 was employed with a resulting layer thickness of  $65 \pm 3 \mu\text{m}$  and a theoretical ink volume of  $24.4 \text{ cm}^3 \text{ m}^{-2}$ . The sheet resistance was measured to be about  $2 \text{ k}\Omega/\square$ . The gate electrode was also chosen to be PEDOT:PSS to avoid any electrochemical effects and to keep the design simple. It was printed orthogonally 1 mm away from the source-drain channel on an effective area of 2 mm  $\times$  1 mm. Ag electrodes were subsequently deposited on the source, drain and gate contacts using a mesh rating of 61/64 resulting in a layer thickness of about  $100 \pm 5 \mu\text{m}$  and a theoretical ink volume of  $30.4 \text{ cm}^3 \text{ m}^{-2}$ . The sheet resistance was subsequently measured to be less than  $1 \Omega/\square$ .



The printed gate electrode was isolated from the source-drain channel via an electrolyte containing 0.15 mM PBS with a pH controlled to 7.4. This electrolyte was physically contained in a well formed by an extension of the PET substrate folded over and hot-laminated over the source-drain-gate area. A laser-cut hole (effective area of 9 mm × 7 mm) was made in the centre of the PET extension (figure 1) during the preparation of the substrate before printing. This ensured that the electrolyte containing the enzyme and the analyte was always contained within the active area to avoid spillage (figure 2).

The well was filled with 50  $\mu$ l of 500 units/ml  $GO_x$  solution in PBS until electrochemical stability. Subsequently different concentrations of glucose were introduced and the drain current modulations recorded at constant gate voltage of 0.6 V D.C (figure 5(A)). Original characterization was done using a Keithley 2400 Source-Measure unit and an EXTECH instruments EX505 low current measurement unit.

The final integrated measurement system employed a transimpedance amplifier designed around Texas Instruments' LM358DR operational amplifier [16]. The current to voltage conversion allowed for an easy measurement in micro to nanoampere range which was ideally suited for biosensing purposes. The drain and gate voltages were supplied via the CAT102 precision

adjustable shunt regulator with a 600 mV reference voltage [17]. The communication and processing was achieved via an 8 bit, 32 pin ATMEGA328PB-AUR microcontroller [18] with 10 bit ADC and an operating voltage range of 1.8–5.5 V, showcasing a power-down mode current of about 200 nA. Two CR2016 button cells were used as power sources.

### 3. Results and discussion

Prior to the fabrication of the fully integrated sensor with CMOS components, the biosensor was fabricated independently (figure 1) and characterization was performed under controlled conditions. Sensitivity and drain current modulations were plotted respectively to attain parameter values relevant for the CMOS circuit design. Sensitivity of the biosensor was ascertained from the slope of the drain current ( $I_d$ ) v/s the glucose concentration ( $C_g$ ) plot (figure 3). The sensitivity for varying gate voltages are shown in table 1.

A gate voltage of 0.6 V showed increased sensitivity and was low enough to circumvent electrolysis effects. This result was implemented in the design of the electronic circuitry for measuring glucose concentrations from the biosensor's drain current modulation.

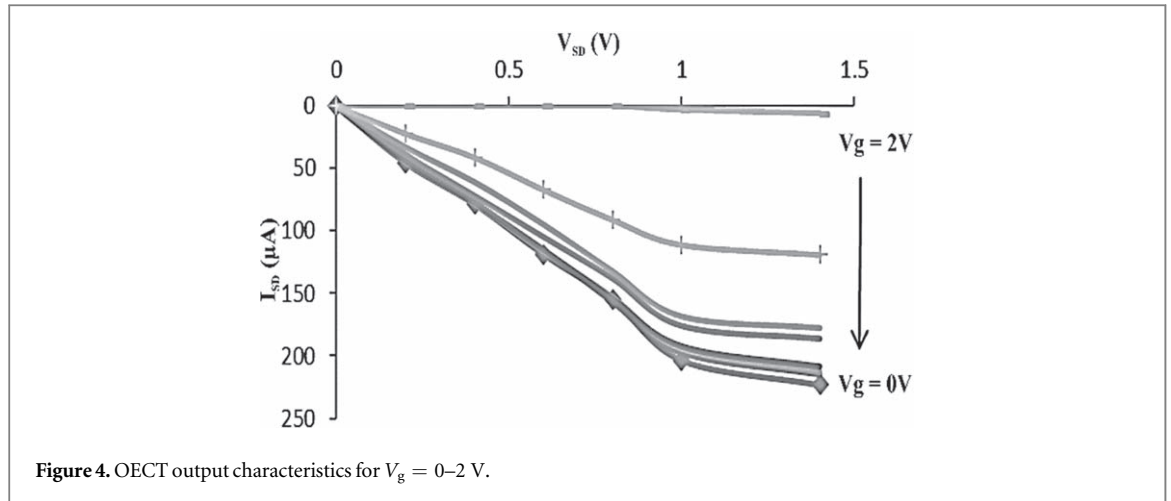


Figure 4. OECT output characteristics for  $V_g = 0\text{--}2\text{ V}$ .

Table 1. Sensitivity of the biosensor for varying gate voltages.

Sensitivity ( $\mu\text{A cm}^{-2} \text{ mM}^{-1}$ )	Gate voltage (V)
0.48	0.2
0.49	0.3
0.54	0.6
0.54	0.8

A figure of merit for transistor gain was also identified by ascertaining the transconductance ( $g_m$ ) from the output curves (figure 4).

A transconductance value of 0.3 mS was obtained. This is in good agreement with previous reports and 20 times higher than similar although more technically sophisticated sensors employing electrolyte immobilization techniques [13].

Figure 5(A) shows the response of the device towards successive additions of varying glucose concentrations. A clear current modulation can be seen between concentration ranges varying within 0.001 and 10 mM. The error bars show a tendency of the biosensor to saturate after the 10 mM concentration range which shows good agreement with previous reports on linear range [19, 20].

The detection limit of 0.001 mM ( $1\ \mu\text{M}$ ) arrived at herein however can be lowered further by a factor of 10 to  $0.1\ \mu\text{M}$  via gate electrode functionalization [20] or down to 30 nM by using alternate positively charged (PANI) and negatively charged (Nafion/Graphene) bilayers at the gate electrode [8, 21]. However, for the purposes of detecting hyper/hypoglycemia, a glucose sensitivity ranging between 0.001 and 10 mM seems sufficient especially since human saliva glucose levels range between 0.008 and 0.2 mM [22, 23]. Additionally, blood glucose levels in healthy non-diabetic individuals range between 4 and 8 mM [15, 23], while diabetic patients' glucose levels range between 2 and 30 mM [15].

Figure 5(B) shows the Normalized Response of the source-drain current as a function of applied gate

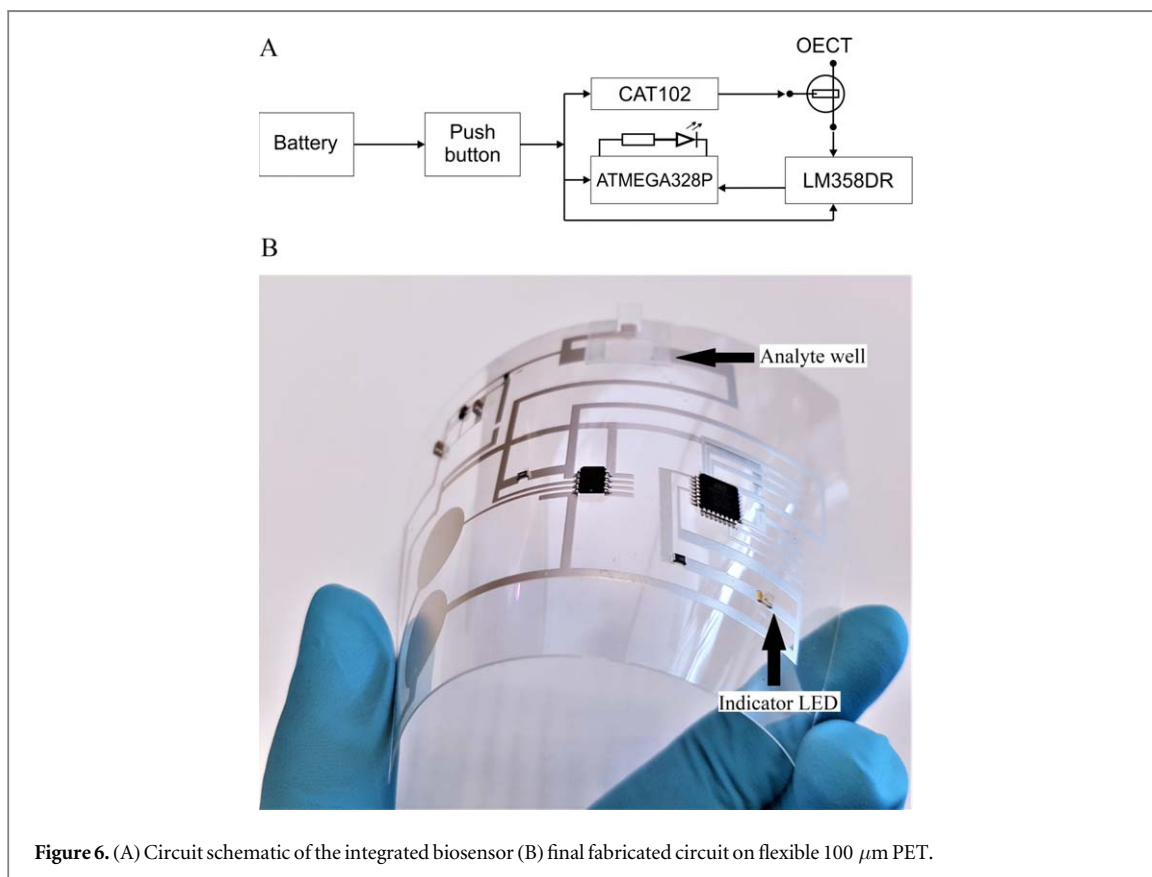
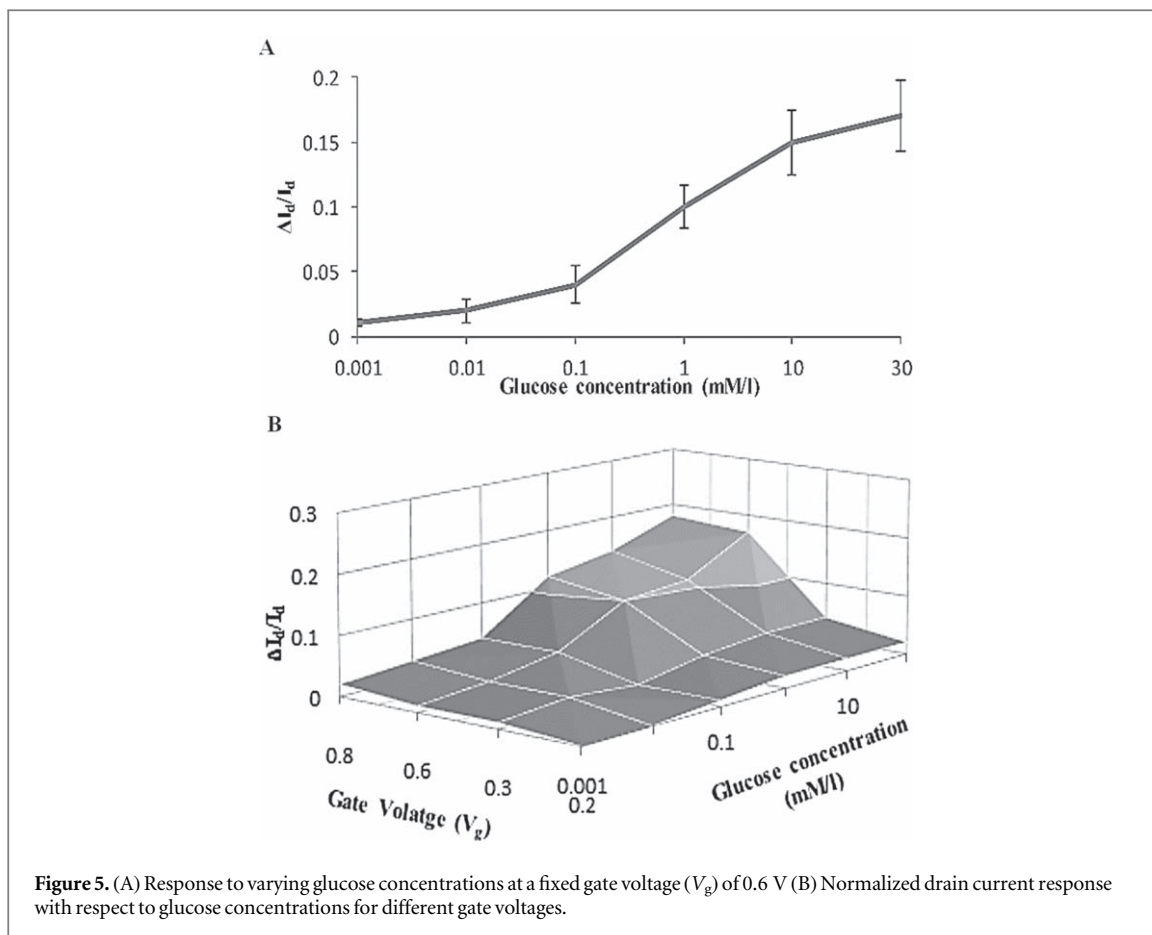
voltage and glucose concentration in a grid format and conforms well with previous simulations [24]. The response time of the biosensor was close to 8 s which is preferable for a portable sensing device compared with reports utilizing immobilized enzymes wherein the response time can be in minutes [2]. The aforementioned response to glucose concentrations ranging between 0.001 and 10 mM, demonstrated a feasibility of measuring in-vitro drain current modulations in response to human saliva under fasting conditions. Normalized response (NR) of the biosensor was found using the following relation:

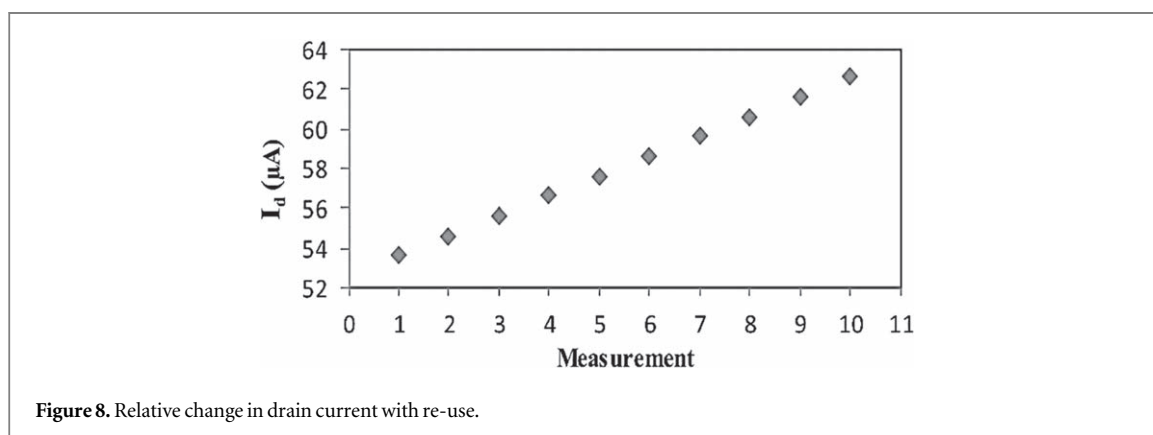
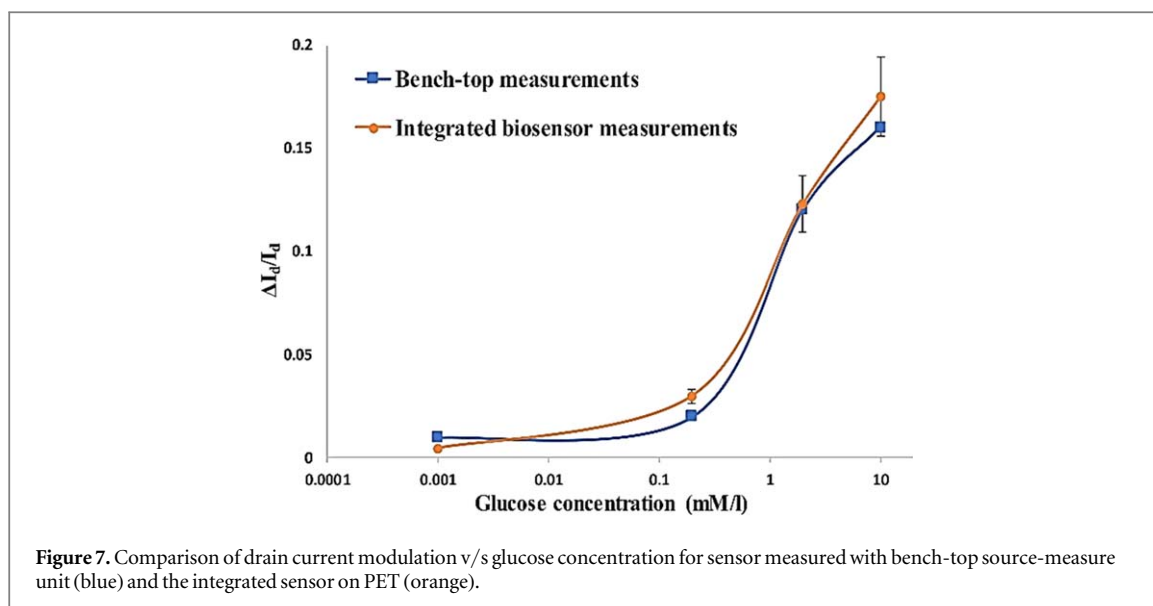
$$\left( \frac{\Delta I_d}{I_d} \right) = \left| \frac{I_d^{\text{Glucose}=0} - I_d^{\text{Glucose}=x}}{I_d^{\text{Glucose}=0}} \right|, \quad (1)$$

where  $I_d^{\text{Glucose}=0}$  is the drain-current when there is no glucose present in the electrolyte solution while as  $I_d^{\text{Glucose}=x}$  is the drain current when glucose of a certain concentration— $x$ , is added to the electrolyte solution at a gate voltage of interest. Measurement of the sensor's drain current as a Normalized Response allowed for the comparison of different samples with respect to the calibrated values stored within the microcontroller.

The operational procedure of the fully integrated biosensor circuitry (figure 6) was programmed into the microcontroller and the custom source-code was written in C++. The algorithm utilized was executed in the following sequence:

(i) At power-on, CAT102 supplies power to the biosensor (ii) the drain current,  $I_d^{\text{Glucose}=0}$  is sensed by the transimpedance amplifier and fed into the 10 bit ADC of the microcontroller and subsequently stored in memory, (iii) the biosensor is now ready to receive the analyte for measurement, indicated by a blinking led (iv) upon addition of glucose, the microcontroller interprets any change in the input to its ADC pin as the detection of the analyte— $I_d^{\text{Glucose}=x}$ , (v) a delay of 10 s allows the reading to stabilize following which the Normalized Response (NR) is calculated (vi) The value is compared with calibrated data and an LED is turned-on if the value exceeds a certain threshold.





Data obtained from the biosensor was now plotted against that obtained from original bench-top measurements. Figure 7 shows the comparison of data recorded with the two setups at 0.001, 0.2, 2 and 10 mM glucose concentrations.

Response of the integrated sensor was comparable to that obtained from more accurate bench-top instruments. Five of the best samples were selected and standard deviation from averaged measurements showed an increase in variation at higher analyte concentrations. This may be caused by variations in channel resistance due to inherent imperfections in layer deposition (for example due to solvent evaporation) which, as the drain current reduces in response to higher glucose concentrations, may result in a larger error bar. Measurements of close to 300 samples with 15 OECTs printed simultaneously on a single substrate at a time showed an average variation of 10% with respect to channel resistance.

The above results show that the sensor is capable of differentiating between 0.008 and 0.2 mM glucose concentrations once the experimentally ascertained calibration curve is extrapolated to within a suitable range and uploaded onto the microcontroller. This opens up avenues for simple non-invasive, in-vitro glucose monitoring. Saliva glucose, for example,

exceeding 0.2 mM at fasting would indicate hyperglycemia while any reading below the 0.008 mM mark would indicate hypoglycemia without a need to accurately measure intermediate values. Any indication of either state can dictate the individual to seek professional medical advice.

Figure 8 shows the drain current response of the sensor upon reuse, clearly indicating partial irreversible reduction of the semiconducting channel which gives credence to the aim of fabricating high throughput, inexpensive, single use/use-and-throw printed functional devices.

#### 4. Conclusion

In conclusion, a fully integrated, hybrid biosensing system on a flexible plastic substrate for the measurement of physiologically relevant quantities of glucose to detect hypo/hyperglycemia using saliva is demonstrated. An effort has been made to improve the state of the art in printed biosensing by demonstrating fully printed sensors fabricated in ambient conditions and overcoming the reliability related issues inherent to conventional mass-printed sensors by implementing a

CMOS circuit topology to ascertain a Normalized Response. The printed OECT based on PEDOT:PSS channel and gate used no redox mediators and the integrated platform demonstrated satisfactory sensitivity to glucose concentrations concurrent with human saliva and blood. The system also has the potential to be powered using printed batteries or NFC signals from smartphones. An inexpensive, disposable label and a reusable encapsulated reader such as this can allow conventional printerries to actively mass-produce over-the-counter biosensors en-masse.

## Acknowledgments

The author would like to thank Dr Moazzam Ali (CEO Saralon GmbH) and Prof. Dr-Ing. Arved Carl Hübler (Department of Print and Media Technology, Technical University of Chemnitz), Germany for support and guidance.

## ORCID iDs

Rakesh Rajendran Nair  <https://orcid.org/0000-0003-3295-6675>

## References

- [1] IDF Diabetes Atlas 2017 8 International diabetes Federation
- [2] Scheiblin G, Aliane A, Strakosas X, Curto V F, Coppard R, Marchand G, Owens R M, Mailley P and Malliaras G G 2015 *MRS Commun.* **5** 507–11
- [3] Zhu Z T, Mabeck J T, Zhu C, Cady N C, Batt C A and Malliaras G G 2004 *Chem. Commun.* **1556–7**
- [4] Thackeray J W and Wrighton M S 1986 *J. Phys. Chem.* **90** 6674–9
- [5] He R X, Zhang M, Tan F, Leung P H M, Zhao X Z and Chan H L W 2012 *J. Mater. Chem.* **22** 22072–6
- [6] Krishnamoorthy K, Gokhale R S, Contractor A Q and Kumar A 2004 *Chem. Commun.* **820–1**
- [7] Gualandi I, Marzocchi M, Scavetta E, Calienni M, Bonfiglio A and Fraboni B 2015 *J. Mater. Chem. B* **3** 6753–62
- [8] Benoit P, Giorgio M, Samia Z, Guillaume A, Nicolas B, Dany C, Antoine M and Steve R 2018 *Appl. Sci.* **8** 928
- [9] Liao C 2014 *M. Phil. Thesis* The Hong Kong Polytechnic University (<https://theses.lib.polyu.edu.hk/bitstream/200/7528/2/25805.pdf>)
- [10] Liu J, Agarwal M and Varahramyan K 2008 *Sensors Actuators B* **135** 195–9
- [11] Kanakamedala S K, Alshakhouri H T, Agarwal M and DeCoster M A 2011 *Sensors Actuators B* **157** 92–7
- [12] Liao J, Si H, Zhang X and Lin S 2019 *Sensors* **19** 218
- [13] Scheiblin G, Aliane A, Strakosas X, Curto V F, Coppard R, Marchand G, Owens R M, Mailley P and Malliaras G G 2015 *MRS Commun.* **5** 507–11
- [14] Zhu Z T, Mabeck J, Zhu C, Cady N C, Batt C A and Malliaras G G 2004 *Chem. Commun.* **13** 1556–7
- [15] Heller A 1999 *Annu. Rev. Biomed. Eng.* **01** 153–75
- [16] Texas Instruments 2019 Industry-standard dual operational amplifiers LM358 Datasheet
- [17] 2009 Precision, adjustable shunt regulator(600 mV reference) CAT102 Datasheet (<https://mouser.de/datasheet/2/308/CAT102-D-108999.pdf>)
- [18] 2015 AVR microcontroller with core independent peripherals and PicoPower technology ATmega328PB datasheet (<http://microchip.com/downloads/en/DeviceDoc/40001907A.pdf>)
- [19] Liao J, Lin S, Yang Y, Liu K and Du W 2015 *Sensors Actuators B* **208** 457–63
- [20] Yang S Y, Cicoria F, Byrne R, Benito-Lopez F, Diamond D, Owens R M and Malliaras G G 2010 *Chem. Commun.* **46** 7972–4
- [21] Liao C, Mak C, Zhang M, Chan H L and Yan F 2015 *Adv. Mater.* **27** 676–81
- [22] Yamaguchi M, Mitsumori M and Y *IEEE Eng. Med. Biol.* **17** 59
- [23] Kanakamedala S K 2011 *Doctoral Dissertation* Louisiana Tech University (<https://digitalcommons.latech.edu/dissertations/366>)
- [24] Bernards D, Macaya D, Nikolou M, DeFranco J, Takamatsu S and Malliaras G 2008 *J. Mater. Chem.* **18** 116–20